Proceedings of the ASME 2020
14th International Conference on Energy Sustainability
ES2020
June 8-10, 2020, Denver, CO, USA

SAND2020-5572C

ES2020-1607

FINITE ELEMENT ANALYSIS OF A MOVING PACKED-BED PARTICLE-TO-sCO_2 HEAT EXCHANGER TESTING AND PERFOMANCE

Nicolas A. DeLovato[1], Kevin J. Albrecht, Clifford K. Ho
Concentrating Solar Technologies Department,
Sandia National Laboratories
Albuquerque, NM

ABSTRACT

A focus in the development of the next generation of concentrating solar power (CSP) plants is the integration of high temperature particle receivers with improved efficiency supercritical carbon dioxide (sCO_2) power cycles. The feasibility of this type of system depends on the design of a particle-to-sCO_2 heat exchanger. This work presents a finite element analysis (FEA) model to analyze the thermal performance of a particle-to-sCO_2 heat exchanger for potential use in a CSP plant. The heat exchanger design utilizes a moving packed bed of particles in crossflow with sCO_2 which flows in a serpentine pattern through banks of microchannel plates. The model contains a thermal analysis to determine the heat exchanger's performance in transferring thermal energy from the particle bed to the sCO_2. Test data from a prototype heat exchanger was used to verify the performance predictions of the model. The verification of the model required a multitude of sensitivity tests to identify where fidelity needed to be added to reach agreement between the experimental and simulated results. For each sensitivity test in the model, the effect on the performance is discussed. The model was shown to be in good agreement on the overall heat transfer coefficient of the heat exchanger with the experimental results for a low temperature set of conditions with a combination of added sensitives. A set of key factors with a major impact on the performance of the heat exchanger are discussed.

Keywords: Heat Exchanger; Concentrating Solar Power; Thermal Simulation

NOMENCLATURE

APW	average particle width
BPV	bulk particle velocity
C	particle bed conductance
CFD	computational fluid dynamics
CSP	concentrated solar power
FEA	finite element analysis
h_{nw}	temperature dependent near wall conductance
HX	heat exchanger
k	thermal conductivity (W/m-K)
LF	loose fill
$\dot{m}$	mass flow rate
q_w	heat flux from the particle bed to the plate
SB	static bed
sCO_2	supercritical carbon dioxide
T_p	particle bed temperature
T_{CO_2}	sCO_2 temperature
U	overall heat transfer coefficient

Greek Symbols

ΔT_{lm}	log mean temperature difference

INTRODUCTION

Particle receivers have been identified as a promising technology for CSP with good potential for commercial application [1]. Another encouraging technology for CSP is the sCO_2 Brayton power cycle. The integration of this power cycle with CSP can offer high thermal-to-electric efficiency and reduce power generation costs [2, 3]. The combination of these technologies could result in significant cost reduction of CSP leading to high penetration of this renewable energy source. Implementation of particle-based CSP relies on the development of a particle-to-sCO_2 heat exchanger to effectively transfer heat from the particle bed to the sCO_2 power cycle. A significant area of focus for heat exchangers is the development of a computation model capable of predicting thermal performance. A robust heat exchanger performance model is essential in the transition from small-scale experimental tests to large-scale commercial applications through accurately sizing and costing equipment. Economic viability is vital for CSP to become a prominent technology for power generation.

Figure 1 shows the moving packed-bed particle-to-sCO_2 heat exchanger modeled in this study. The particle flow is introduced at the top of the heat exchanger and flows in channels between the plates of each bank driven by gravity. While flowing through the heat exchanger, the particle bed is separated into

[1] Contact author: ndelova@sandia.gov

individual channels between the parallel plates and recombines to a single stream before exiting the heat exchanger. The sCO_2 flows in a serpentinite pattern upwards through three banks of parallel plates by moving locally in cross flow and then traveling up to the next bank through the external piping as shown in Figure 1. In each bank, the sCO_2 is distributed to the individual plates through headers which are welded to the plate edges and feed the microchannels of each plate. The sCO_2 recombines in the header on the opposite side of the plate after exiting the microchannel network and is then routed to the next bank in series.

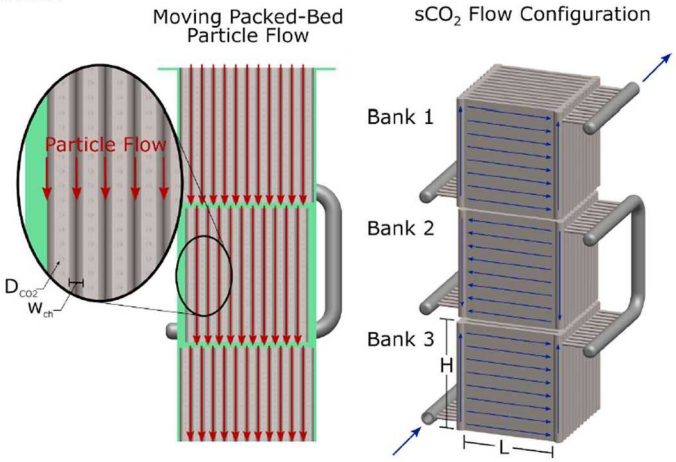

Figure 1. Overview of a moving packed-bed particle-to-sCO_2 shell-and-plate heat exchanger [4].

Previous models of moving packed-bed heat exchangers in the literature have been mostly low-dimensional models (1D or 2D) and focused on single application [4-6]. Baumann and Zunft [5] recently presented a CFD model on the hydrodynamics of a moving packed-bed heat exchanger, but it lacked a thermal analysis to predict the heat exchangers performance. Albrecht et al. [6] developed a 1D model for a moving packed-bed heat exchanger, which can predict the performance effects of a variety of parameters. In addition to this model, further modeling is needed to provide more detailed analysis by accounting for localized phenomena through representing the entire 3D geometry. This paper details the development of a FEA model which predicts the thermal behavior of a moving packed-bed particle-to-sCO_2 heat exchanger by resolving the full 3D geometry. In addition, the developed model is exercised in a sensitivity analysis and verified against experimental data.

NUMERICAL MODEL

The FEA model used in this study was initially developed for the shell-and-plate moving packed-bed heat exchanger design detailed by Ho et. al [7]. The model was then modified to capture the geometry of the as-built shell-and-plate heat exchanger illustrated in Figure 1. The layout of the computational domain for the model is shown in Figure 2.

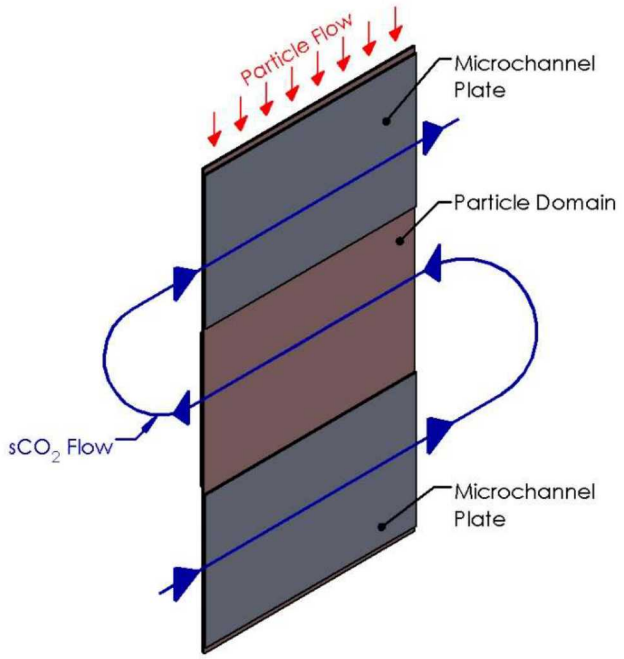

Figure 2. Illustration of the interbank coupling and computational representation of the shell-and-plate moving packed-bed heat exchanger

The particle bed is modeled as a continuum using the advection-diffusion equation with a prescribed, uniform velocity. The sCO_2 flow through the hundreds of microchannels is modeled using one-dimensional advective bar elements located at the center of all the microchannels to capture the sCO_2 flow distribution without requiring a full CFD simulation. The one-dimensional sCO_2 channel models are coupled to the three-dimensional plate geometry through a heat transfer correlation. Thermal contact resistance is utilized to represent the reduced thermal conductivity between the particle bed and the microchannel plate. The heat flux between the particles and the plate is determined by equation (1). Where C is the conductance of the particle bed, T_1 and T_2 are the temperatures of the surfaces in contact, and q_w is the heat flux supplied to the plate by the particle bed.

$$q_w = C(T_1 - T_2) \quad (1)$$

The results of the model have been verified through checking the conservation of energy by comparing the mass-weighted average enthalpy of the sCO_2 at the microchannel outlets with the average enthalpy of the particle bed at its outlet. The model simulates the multiple banks of the heat exchanger by coupling the inlet temperature boundary conditions of the sCO_2 channels at the plate bank above to the mixed outlet temperature of the plate bank below. Refer to Figure **2** for the relation between the plate banks. This transfer was done by taking the mass-weighted sCO_2 enthalpy average of the bottom plate, then converting this enthalpy into temperature, and applying this temperature to the inlet of the next plate. The conversion between enthalpy and temperature was required due to the highly

variable properties of sCO_2. The model uses temperature-dependent sCO_2 properties for density, thermal conductivity, and viscosity.

The main objective of the heat exchanger model is to predict the overall heat transfer coefficient (U) of a prototype heat exchanger to provide confidence in use for scale-up. The calculation of the overall heat transfer coefficient is done using equations (2) and (3). Where ΔT_{lm} is the log-mean temperature difference, A_s is the total area of the plate surfaces in contact with the particle bed, and Q is the total heat transferred from the particle bed to the sCO_2.

$$\Delta T_{lm} = \frac{\left(T_{p,out} - T_{CO_2,in}\right) - \left(T_{p,in} - T_{CO_2,out}\right)}{\ln\left(\frac{T_{p,out} - T_{CO_2,in}}{T_{p,in} - T_{CO_2,out}}\right)} \quad (2)$$

$$U = \frac{Q}{A_s \Delta T_{lm}} \quad (3)$$

FEA SENSITIVITY STUDIES

The predicted performance by the baseline model (122 W/m^2-K) varied drastically from the performance results from the experimental tests (66.6 W/m^2-K). Several sensitivity analyses were performed using the model, detailed in Table 1, to identify the possible areas where the numerical and experimental results deviate. This sensitivity test was focused around a single experimental data point to decrease computational demand. However, future studies will look to validate the model over the entire operating envelope of the heat exchanger.

Table 1. Sensitivities Tested in the FEA Model.

Test Case	Description
Average Particle Width	Particle channel width is increased to the total particle width divided by number of plates.
Bulk Particle Velocity	A bulk particle velocity is used in two simulations for the differing particle widths.
CFD $\dot{m}$	sCO_2 mass flow rates used in advective bars are based on CFD analysis of sCO_2 plate.
Double	A double particle bed with and half-plate on both side with sCO_2 flow moving in opposite directions on each side of the particle bed.
Double-shifted	Same as double, but with sCO_2 flow moving to the plate on the other side of the particle bed to which it exited from.
Loose Fill Thermal Conductivity	Set particle conductivity to a reduced temperature dependent function based on the nature of a flowing bed.
Headers	Added headers to all the plates of the geometry from the double case with stagnate particle domains in between the headers.
Inline	A single set of plates with the symmetry condition at the center of the particle bed.
Isolated Flow	sCO_2 flow isolated to the shortest flow path between the inlet and outlet nozzle.
Particle flow variation	Linearly varied the advection velocity of the particle bed in two different directions.
sCO_2 flow variation	Linearly varied the mass flow rate of sCO_2 in each channel by a certain percentage.
Single	Base case with a single set of three plates with two on one side and one on the other side of the particle bed.
Plate Bank Spacing	Reduced height of particle space between banks of the heat exchanger.

Decreased Particle Conductivity

The conductivity of the packed particle bed is known to be one of the most significant factors affecting the performance of the heat exchanger. The static bed thermal conductivity for sintered bauxite material was initially used in the model but thought to possibly be an overestimation since the particle bed has a reduced solids volume fraction when in a flowing state. A reduced thermal conductivity based on the flowing volume fraction was evaluated using the model. The loose fill thermal conductivity reduced the overall heat transfer coefficient by around 12% but a sizable difference remained between the simulation and experimental results. The effect of thermal conductivity on the overall heat transfer coefficient was further investigated by reducing thermal conductivity by a fraction for both static bed and loose fill conditions until agreement with the experimental data was achieved. All the functions of thermal conductivity used in this test are shown in Figure 3.

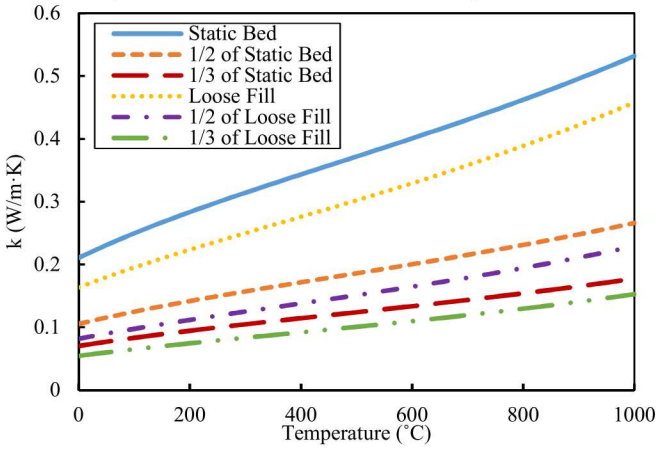

Figure 3. Thermal conductivity as a function of temperature for static and loose fill fractions used in the heat exchanger model

For either value of thermal conductivity, a fraction of one-third was required for agreement with the experimental data as shown in Figure 4. This reduction of thermal conductivity was determined to be unrealistic for the moving packed-bed and thus the thermal conductivity of the particle bed was not the sole reason for the difference. The loose fill thermal conductivity was implemented into the model as it produced a reduction in overall heat transfer coefficient while being realistic to the nature of the moving particle bed.

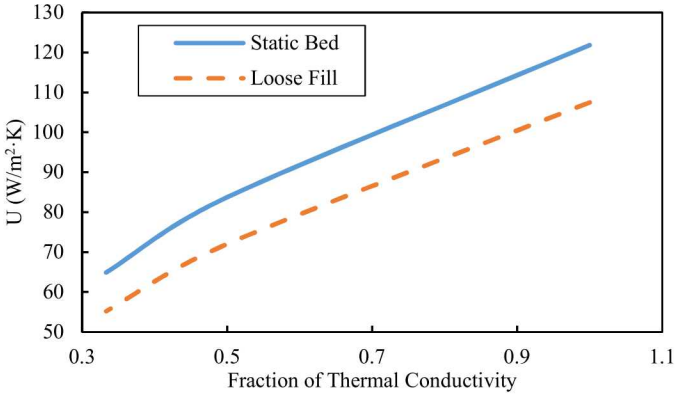

Figure 4. Modeled overall heat transfer coefficient as a function of reduced thermal conductivity

Increased Near Wall Resistance

The thermal resistance between the particle bed and the heat exchanger plate can have a large effect on the performance of a heat exchanger with narrow particle channels. The contact conductance coefficient, C in equation (1), is used to represent the decreased solid volume fraction and reduced thermal conductivity in the near-wall region. This coefficient is thus equal to the inverse of the thermal resistance between the plate wall and the particle bed. The first investigation in this sensitivity study was to set the contact conductance coefficient to the temperature dependent function. This function varies the conductance over the range of 650-2618 W/m^2-K and calculates the conductance at the average of temperatures on the surfaces in contact. Parametric runs were conducted with the near wall conductance calculated from the static bed and loose fill thermal conductivity and it reduced the overall heat transfer coefficient slightly. By only changing the near-wall conductance, the overall heat transfer coefficient was reduced by around 3%. To better understand the effect of the near-wall conductance on overall heat transfer coefficient, the near wall conductance was decreased until agreement was achieved. The results of all the contact conductance coefficient tests are shown in Figure 5. Agreement required the thermal conductance to decrease to unreasonable levels, thus it was determined the near-wall resistance was not the sole case of the difference between modeled and experimental data. The temperature dependent near-wall conductance was incorporated into the model as it reduced the overall heat transfer coefficient while better representing the physics of the heat exchanger in the model.

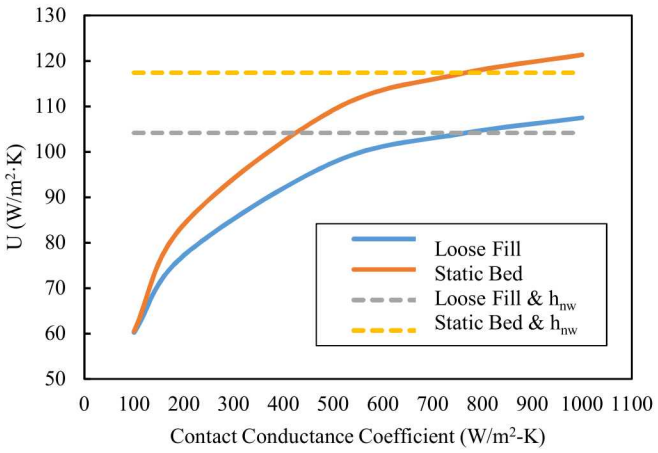

Figure 5. Sensitivity of the overall heat transfer coefficient to contact conductance coefficient

Staggered Plates

Plate staggering can improve the thermal performance of the heat exchanger by disrupting the thermal boundary layer. The initial state of the model contains the half plates staggered on both sides of a half-width particle domain. Test simulations were conducted with the half plates inline on the same side of the particle domain and with a double set of half plates with a full particle domain. An illustration of the geometries is shown in Figure 6. The vertical spacing between the plate banks is investigated in a future section.

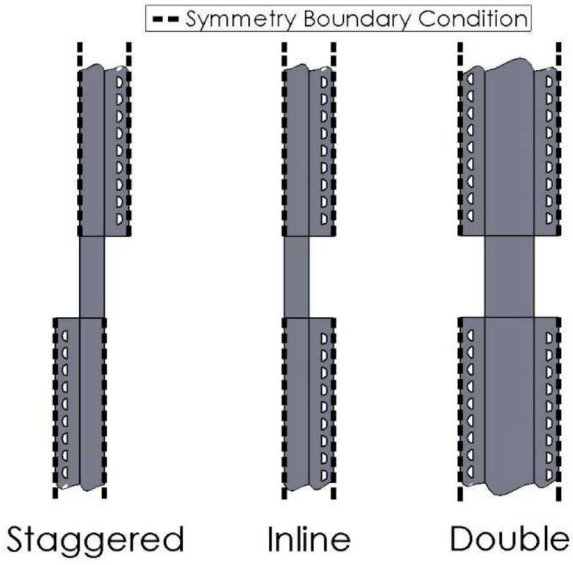

Figure 6. Illustration of the model domain for capturing staggered plates, inline plates, and inline plates with multiple flow paths

The overall heat transfer coefficient was reduced for the inline case by around 1.5%, around 2% for the vertical spacing between plates test, and 1.5 % for the double plates test from the staggered configuration. All these tests resulted in approximately the same reduction in the overall heat transfer coefficient. Thus,

to best represent the as-built heat exchanger geometry, the inline and double configurations were investigated alongside other sensitivities.

Multiple Flow Paths

The double test described in the previous section has the sCO_2 flow up the banks to plates on the same side of the particle domain. The as-built heat exchanger has the sCO_2 shift sides of the particle domain as it moves up to the next bank. This sCO_2 flow path is shown in Figure 7 as 'double shifted' alongside the flow path used in the double test. The double shifted test increased the overall heat transfer coefficient by nearly 1% from the double test. This result signifies that the offset sCO_2 flow paths does not affect the overall heat transfer coefficient.

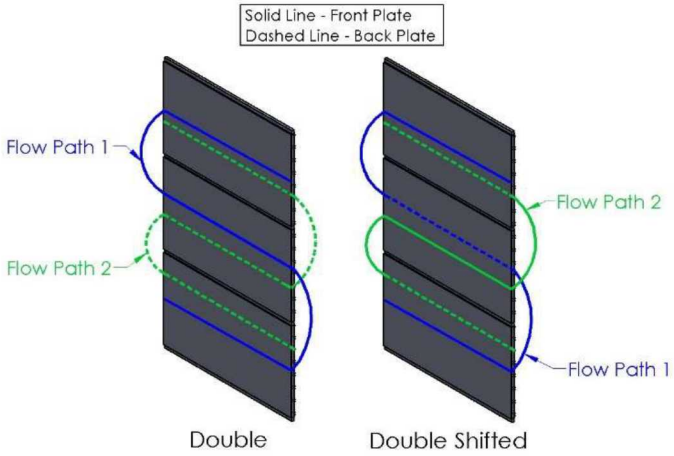

Figure 7. Illustration of two possible cases for the multiple sCO_2 flow paths

Axial Conduction with Headers

Another aspect of the heat exchanger performance that is related to the multiple sCO_2 flow paths is the heat transfer between headers of adjacent plates. The distance between the headers of adjacent plates is less than 3 mm at which the flow of the particle bed stagnates. These stagnant particles between the headers could cause significant heat transfer between the headers which are at different temperatures. The temperature difference of adjacent plates is due to the inlets and outlets of the plates being on opposite sides of the plate (Figure 7). The model was altered by adding headers to the plates in the double configuration with a stagnant particle domain in between the headers as shown in Figure 8. Tied temperature boundary conditions were set for the surfaces where the moving and the stagnant particle domains meet. This boundary condition was also used for the interfaces of the plates and headers. The interface between the stagnant particle domain and the headers was set to have the same as thermal resistance between the moving particle bed and the plates.

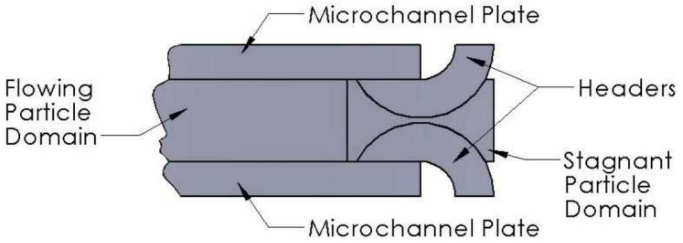

Figure 8. Detailed View of HX Model with Headers.

The overall heat transfer coefficient was reduced by almost 2% and the temperature and heat flux distribution for the case with headers are shown in Figure 9. The small amount of heat transfer between the headers, the slight reduction in overall heat transfer coefficient, and the high computational cost resulted in this modified geometry not being used in future cases.

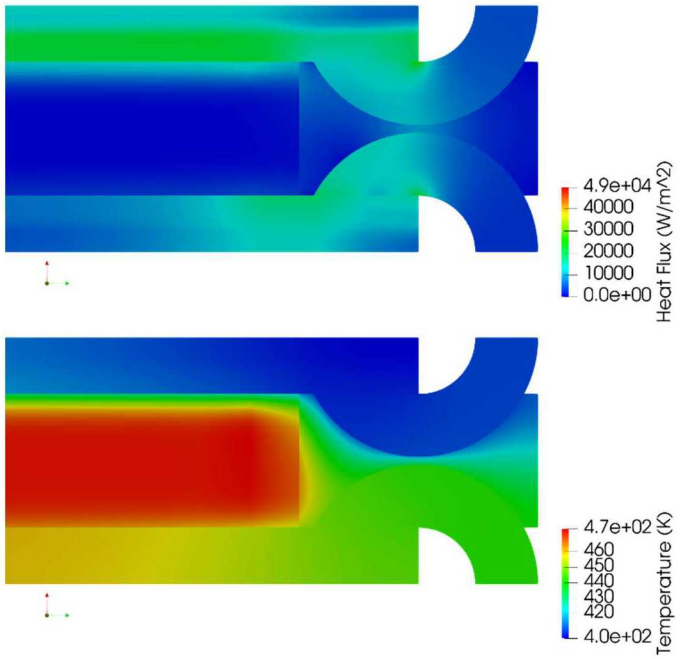

Figure 9. Heat flux and temperature distribution looking at the top surface of the plate with headers (top and bottom respectively).

Particle and sCO_2 Flow Maldistribution

The initial model assumes the velocity of the moving particle bed is spatially uniform. At operating conditions, the true nature of the particle flow within the heat exchanger is difficult to measure, so the particle flow was varied linearly across the length of the plates to determine the effect of the particle flow distribution on the overall heat transfer coefficient. The particle velocity was reduced by half the total amount of variation at one end of the plate and then increased linearly along the plate to where it was increased by half of the total variation at the other end of the plate. The particle velocity was varied in both directions along the plate as shown in Figure 10.

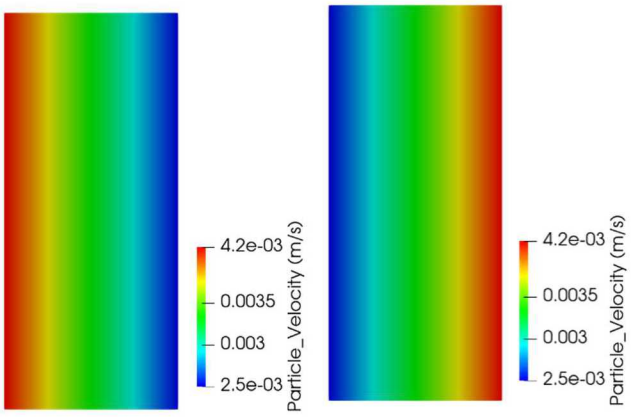

Figure 10. Particle velocity for 50% particle flow variation (positive - left, negative – Right).

The amount of variation of the particle flow reduced the overall heat transfer coefficient by less than 1% for 25%, 50% and 75% flow variation cases. The overall heat transfer coefficient was reduced by around 2.5% for the negative direction. The particle flow is unlikely to have a non-uniformity greater than 75%, thus, the particle velocity was kept constant for further tests.

The effects of sCO_2 flow maldistribution was studied in a similar manner. The sCO_2 flow was varied linearly with the mass flow rate of the top most channel decreasing by half of the total amount of variation and increasing linearly for each channel moving down the plate. The mass flow rate of the bottom most channel was increased by half of the total amount of variation. The sCO_2 flow was varied in this manner as the temperature of the plate is the highest at the top because the particle bed moved from the top to the bottom of the plate. The mass flow rate of each microchannel for this sCO_2 linear flow variation test are shown in Figure 11. The overall heat transfer coefficient was reduced by less than 1% for 25% sCO_2 linear flow variation, around 1.25% for 50%, and around 2.5% for 75%. This large flow variation produced minimal reductions in overall heat transfer coefficient and thus was not investigated in combination with other cases.

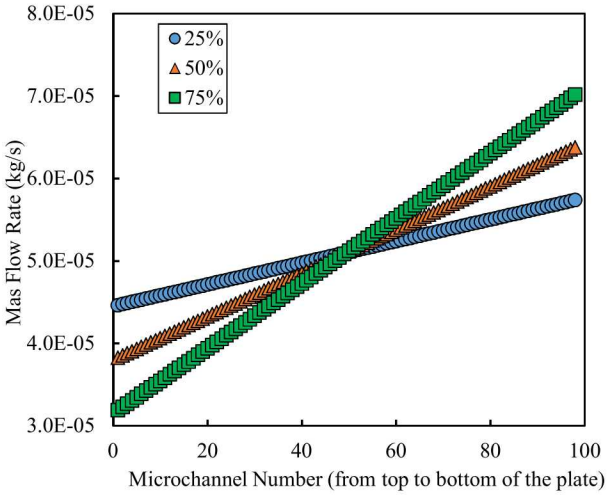

Figure 11. Flow Distribution for sCO_2 Flow Maldistribution Test.

Isolated Channel Flow

The design of the microchannel plates was thought to be possibly isolating sCO_2 flow into certain microchannels that had the shortest flow path between inlet and outlet nozzles. The sCO_2 flows into the header from an inlet nozzle located a distance below the top of the plate. The flow is then separated into the microchannels, then flows into another header before exiting the plate through an outlet nozzle located a distance above the bottom of the plate. A possible result of this design is the sCO_2 flow being isolated in the microchannels located below the inlet nozzle and above the outlet nozzle. The effect of this case was examined in the isolated flow test and is illustrated in Figure 12. The overall heat transfer coefficient was reduced by almost 25% with this test and lead to a CFD analysis of the sCO_2 flow.

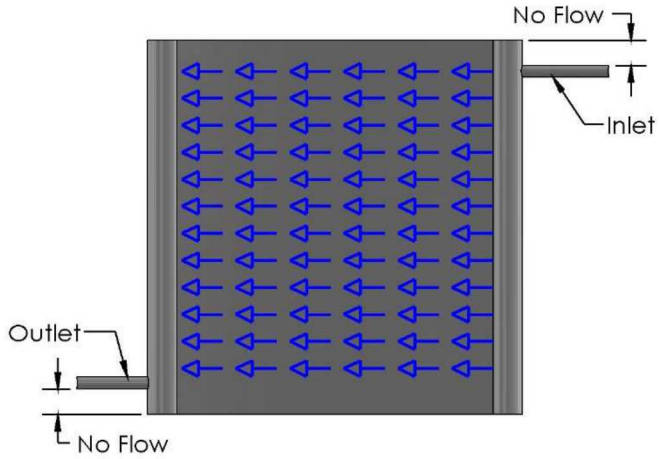

Figure 12. sCO_2 Flow for Isolated Flow Test.

CFD Analysis of sCO_2 Flow

An isothermal CFD analysis of the sCO_2 flow through the plate was completed with ANSYS© Fluent. The k-ε turbulence model was used with material properties of sCO_2 at 100 ˚C and 20 MPa, which was the average sCO_2 temperature

for case A. The velocity distribution of the sCO_2 in the plate is shown in Figure 13 and the mass flow rates of each microchannel is shown in Figure 14. The sCO_2 flow is nearly uniform above the inlet and below the outlet. The mass flow rate is the greatest for the channels aligned with the inlet due to the large stagnation pressure from the high velocity flow from the inlet nozzle, followed by the channels aligned with the outlet. The flow steadily increases from the lowest value in the channel right below the inlet to the channel right above the outlet. This flow distribution was incorporated into the thermal model and resulted in a reduction of overall heat transfer coefficient of around 24%. This significant reduction indicated the importance of the sCO_2 flow distribution, and this sensitivity was studied with additional sensitivities.

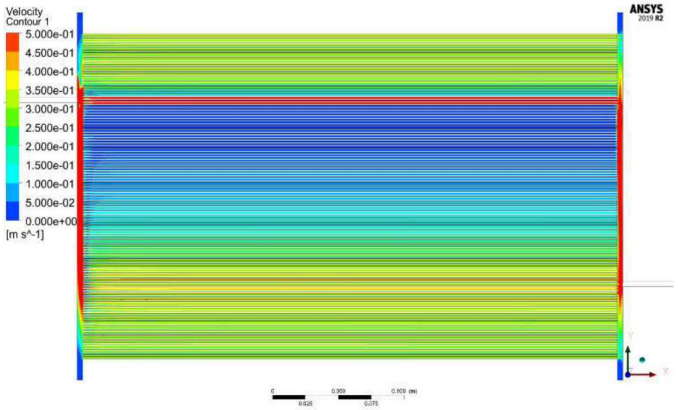

Figure 13. Microchannel sCO_2 velocity distribution at 100 °C and 20 MPa.

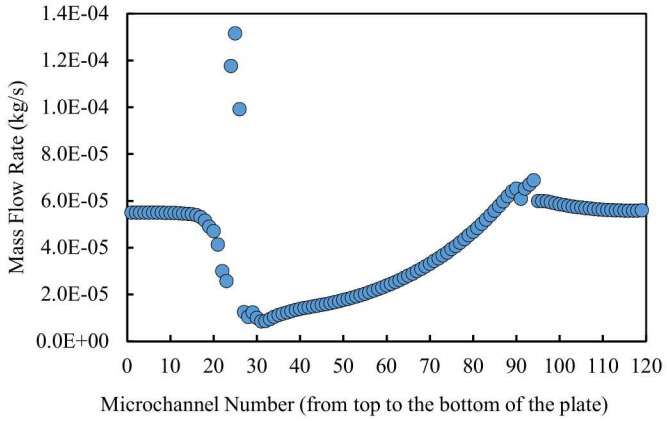

Figure 14. Individual sCO_2 channel mass flow rates at 100 °C and 20 MPa

Average Plate Spacing and Bulk Particle Velocity

For particle containment, the heat exchanger's shell creates a larger area for particle flow between the edge plates and the shell than the area between two plates. This aspect of the heat exchanger is shown in Figure 15. This setup was added to the model by setting the particle domain to an average width. This average was computed by taking the sum of the all the particle channel widths in the heat exchanger divided by the total number of plates. The overall heat transfer coefficient was reduced around 6% with this as-built geometry captured using a particle channel width. This reduction still left a sizable difference so another approach for modeling the additional particle channel width was evaluated.

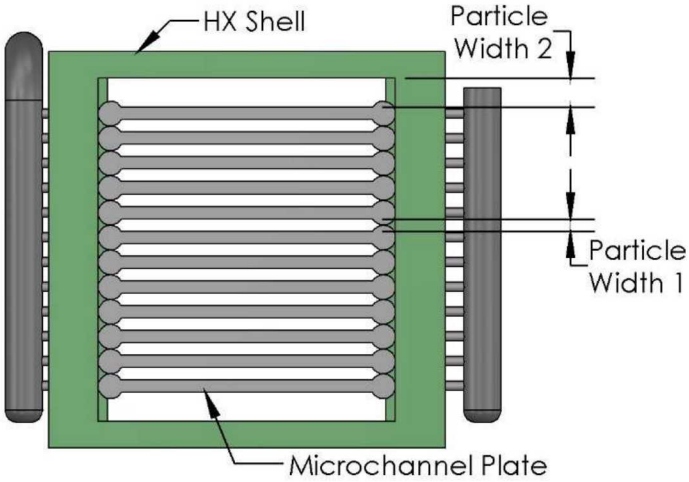

Figure 15. Top view of a bank of the shell-and-plate heat exchanger illustrating the additional space between the last plate bank and heat exchanger case.

A set of two simulations were set up to capture this aspect of the heat exchanger. The first simulation modeled a half-plate with a particle domain of half the space between the plates using a symmetry boundary condition at the centerline of the particle channel. The other simulation was composed of a half-plate with a particle domain the size of the space between the last plate and the heat exchanger shell. Both simulations used a bulk particle velocity which was the velocity calculated from the particle mass flow rate and the particle flow area. Then the mass-weighted average of the enthalpy for both sCO_2 and particle bed was taken from both simulations and used to calculate the outlet temperatures. These outlets temperatures were then used to calculate the overall heat transfer coefficient based on the parameters of the whole heat exchanger. The overall heat transfer coefficient was reduced by around 24% for the bulk particle velocity test and the combination of inline, bulk particle velocity, CFD $\dot{m}$, loose fill thermal conductivity, and h_{nw} sensitives resulted in an error of under 2% between experimental data and simulated performance.

RESULTS

The model of the shell-and-plate heat exchanger was verified with experimental data. Table 2 lists the particle and sCO2 boundary conditions for the model based on the data points collected during the experimental testing. Case A was used as the baselined to understand the discrepancies between the modeled and measured performance described in the previous sections.

Table 2. Conditions modeled for comparison to experimental data.

Test Parameter	Case A	Case B	Case C
Particle inlet temperature	200 ˚C	300 ˚C	400 ˚C
sCO_2 inlet temperature	30 ˚C	100 ˚C	250 ˚C
Particle $\dot{m}$ (kg/s)	0.3784	0.3784	0.4
sCO_2 $\dot{m}$ (kg/s)	0.25	0.3516	0.4265

The results of the sensitivity tests are shown in Figure 16 and Table 3 details the model fidelity for each case. The remaining difference between the simulated and experimental results is an error of less than 1% for the overall heat transfer coefficient. The sensitivity tests resulted in reduction of the overall heat transfer coefficient by around 45% from the initial model-predicted value to the final measured value.

Table 3. Detailed legend for Figure 3.

Change	Plate Arrangement	sCO_2/Particle Flow Distribution	Particle Bed Conductivity	Near Wall Resistance	Edge Effects
Baseline	Staggered Plates	Uniform	Packed Bed	Constant Value	None
1	Double	Uniform	Packed Bed	Constant Value	None
2	Double-shifted	Uniform	Packed Bed	Constant Value	None
3	Staggered Plates	75% sCO_2 and 50% positive particle flow variation	Packed Bed	Constant Value	None
4	Staggered Plates	75% sCO_2 and 50% negative particle flow variation	Packed Bed	Constant Value	None
5	Staggered Plates & Reduced Vertical Spacing	Uniform	Packed Bed	Correlation	None
6	Inline Plates & Reduced Vertical Spacing	Uniform	Packed Bed	Correlation	None
7	Staggered Plates	Uniform	Loose Fill	Correlation	None
8	Inline Plates	Uniform	Loose Fill	Correlation	None
9	Inline Plates	CFD for sCO_2 & Uniform for Particle	Loose Fill	Correlation	None
10	Inline Plates	CFD for sCO_2 & Uniform for Particle	Loose Fill	Correlation	Average Particle Width
11	Inline Plates	CFD for sCO_2 & Uniform for Particle	Loose Fill	Correlation	Two Domains with a Bulk Particle Velocity

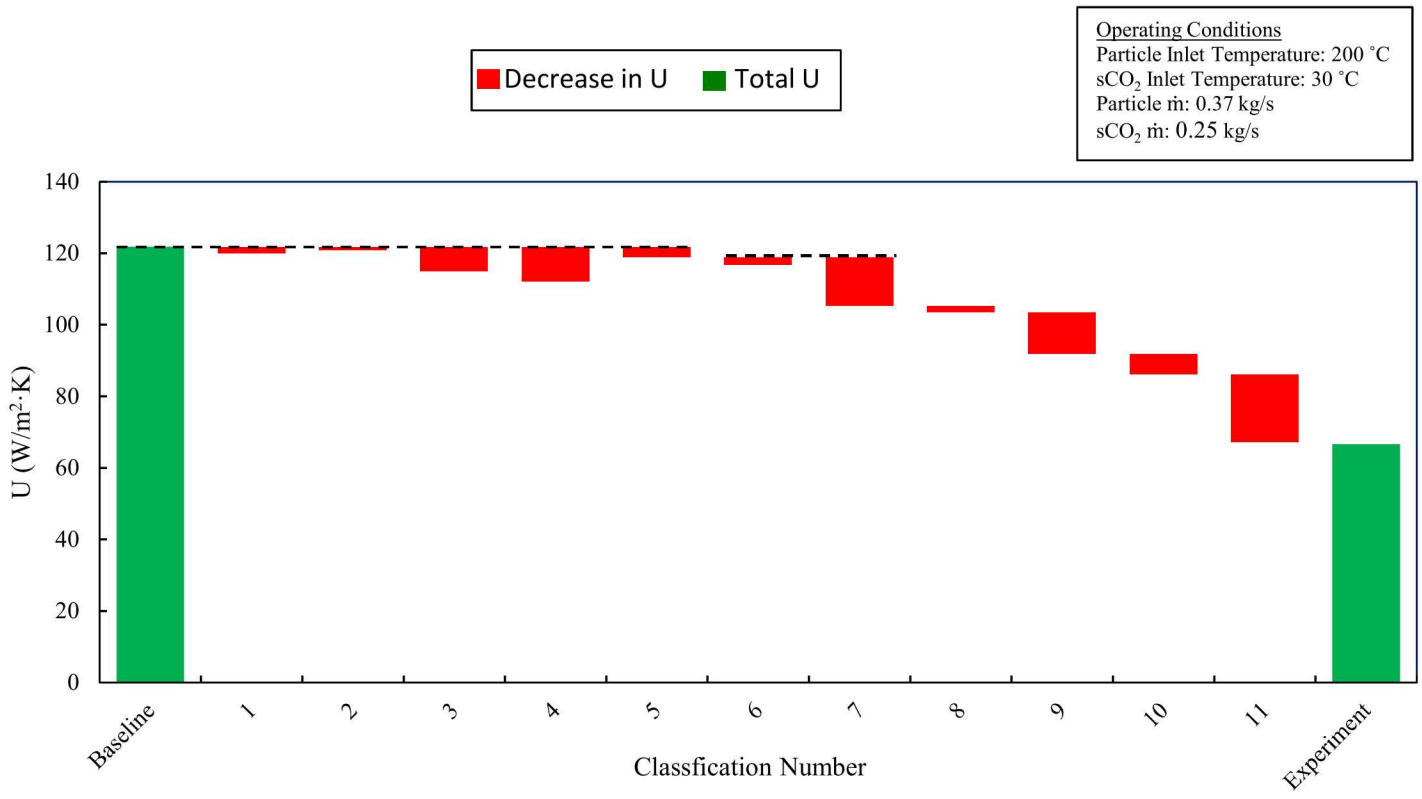

Figure 16. Results of Sensitivity Tests for the Shell-Plate HX Model.

All the sensitivity tests produced a reduction in overall heat transfer coefficient from the base case, but this reduction was only significant for three modifications. The loose fill particle thermal conductivity produced a sizable reduction in overall heat transfer coefficient as a part of number 8. The next large reduction was due to the incorporation of the results of the CFD analysis on the plate sCO_2 flow distribution in number 10. Experimental verification was finally achieved with the largest reduction of overall heat transfer coefficient in number 13 with the dual bulk particle simulations of the heat exchanger. The experimental and simulated results of overall heat transfer coefficient for all the cases shown in are detailed in Figure 17. Case A was aligned through the sensitivity tests, but the difference between the experimental and simulated results reemerged for the other experimental data points. Currently, the model predicts an increase in performance for an increase in the inlet temperatures of the particle bed and sCO_2. The experimental results however show a slight decrease in performance for increasing inlet temperatures for both the particle bed and sCO_2. The effect of this decrease observed in the experimental tests is unknown and further changes to the model are being investigated to determine the cause. However, significant progress has been made to align the model with the experimental results.

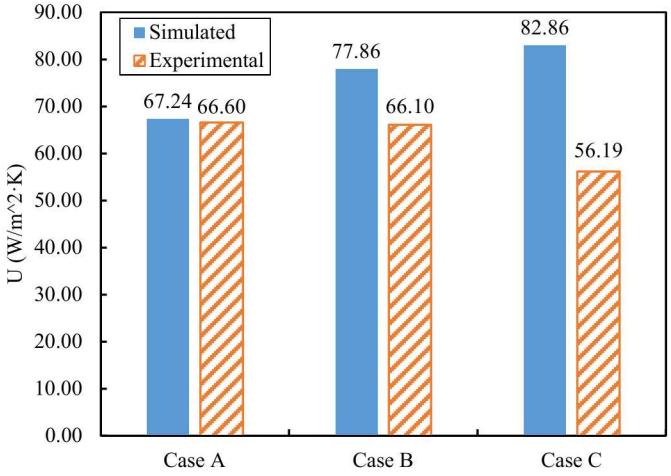

Figure 17. Comparison of results for preliminary cases.

CONCLUSIONS

The development process of a FEA model to predict the performance of a moving packed-bed particle-to-sCO_2 heat exchanger was presented. Through this process several key factors for the performance of the heat exchanger were uncovered. The first important factor identified was the thermal conductivity of the moving packed-bed. In this state, the particle bed has properties in between a packed-bed and fluidized bed, so using the properties of either of these states will produce inaccurate results. It is critical to have accurate values for the

thermal conductivity of the moving packed bed for appropriate predictions of heat exchanger performance.

Another key factor found is the sCO_2 flow distribution through the plate. When sCO_2 is separated into multiple channels it is vital to determine the amount of sCO_2 flowing in each channel. The nature of the sCO_2 flow effects its ability to absorb heat from the particle bed, which substantially effects the performance of the heat exchanger.

The last key factor is the size of the particle domain. When using symmetry to reduce the computational costs of the model, it is important to account for any dissimilarity in the particle bed due to the design of the heat exchanger. The most accurate method to address any dissimilarities is to run separate simulations for each dissimilarity. Then average the enthalpy at the outlets and calculate the performance from those enthalpy averages. Further development of this model will focus on fixing the difference for cases B and C. Once the model is aligned with the experimental test for all cases, a mechanical failure analysis will be added into the model. The goal of this modeling process is to be able to predict the thermal performance of the heat exchanger and if failure occurs for a variety of design iterations. A model with these abilities will be a major asset for the advancement of particle-based receivers and the sCO_2 Brayton power cycle for CSP.

ACKNOWLEDGEMENTS

The paper is based upon work supported in part by the DOE SunShot Program (SuNLaMP-0000000-1507). Sandia National Laboratories is a multimission laboratory managed and operated by National Technology and Engineering Solutions of Sandia LLC, a wholly owned subsidiary of Honeywell International Inc. for the U.S. Department of Energy's National Nuclear Security Administration under contract DENA0003525.

REFERENCES

[1] Jiang, Kaijun, Du, Xiaoze, Kong, Yanqiang, Xu, Chao, and Xing, Ju. "A comprehensive review on solid particle receivers of concentrated solar power." *Renewable and Sustainable Energy Reviews*, Vol. 116 (2019).

[2] Li, Ming-Jia, Zhu, Han-Hui, Guo, Jia-Qi, Wang, Kun, and Tao, Wen-Quan. "The development technology and applications of supercritical CO2 power cycle in nuclear energy, solar energy and other energy industries." *Applied Thermal Engineering* Vol. 126 (2017): pp. 255-275.

[3] Alsagri, Ali Sulaiman, Chiasson, Andrew, and Gadalla, Mohamed. "Viability Assessment of a Concentrated Solar Power Tower With a Supercritical CO2 Brayton Cycle Power Plant." *Solar Energy Engineering* Vol. 141 No. 5 (2019).

[4] Botterill, J.S.M., and Denloye, A.O.O. "A theoretical model of heat transfer to a packed or quiescent fluidized bed." *Chemical Engineering Science* Vol. 33 No. 4 (1978): pp. 509-515.

[5] Park, Sang Il. "Performance analysis of a moving-bed heat exchanger in vertical pipes." *Energy* Vol. 21 No. 10 (1996): pp. 911-918.

[6] Henda, Redhouane and Falconi, Daniel J. "Modeling of Heat Transfer in a Moving Packed Bed: Case of the Preheater in Nickel Carbonyl Process." *Journal of Applied Mechanics* Vol. 73 No. 1 (2006): pp. 47-53.

[7] Baumann, T and Zunft S. "Theoretical and experimental investigation of a Moving Bed Heat Exchanger for Solar Central Receiver Power Plants." *Proceedings of the Sixth European Thermal Sciences Conference*. pp. 1-8, 2012.

[8] Albrecht, Kevin J. and Ho, Clifford K. "Heat Transfer Models of Moving Packed-Bed Particle-to-SCO2 Heat Exchangers," *Journal of Solar Energy Engineering* Vol. 141 (2019).

[9] Albrecht, Kevin J. and Ho, Clifford K. "High-temperature flow testing and heat transfer for a moving packed-bed particle/sCO2 heat exchanger." *AIP Conference Proceedings* Vol. 2033 (2018).

[10] Ho, Clifford K., Carlson, Matthew, Albrecht, Kevin J., Ma, Zhiwen, Jeter, Sheldon, and Nguyen, Clayton M. "Evaluation of Alternative Designs for a High Temperature Particle-to-sCO2 Heat Exchanger," *Journal of Solar Engineering* Vol. 141 (2019): pp. 21001-8.